Magnetic characteristics of synthetic pseudo-single-domain and multi-domain greigite (Fe_3S_4)

Liao Chang,[1] Andrew P. Roberts,[1] Adrian R. Muxworthy,[2] Yan Tang,[3] Qianwang Chen,[3] Christopher J. Rowan,[1] Qingsong Liu,[1] and Petr Pruner[4]

Received 2 October 2007; revised 25 October 2007; accepted 19 November 2007; published 21 December 2007.

[1] We report the magnetic properties of pure synthetic pseudo-single-domain (PSD) and multi-domain (MD) greigite and the grain size dependence of the magnetic properties of greigite for the first time. The dominantly PSD-like and MD-like behavior are demonstrated by hysteresis, first-order reversal curve diagrams, low-temperature cycling (LTC) of room temperature saturation isothermal remanent magnetization (SIRM) and low-temperature SIRM warming curves. Variations in a range of magnetic properties clearly correlate with grain size. Characteristic PSD/MD behavior is preserved at low temperatures, which, coupled with the small decrease in remanence during warming, rule out the presence of substantial superparamagnetic behavior in the studied samples. LTC-SIRM measurements indicate a continuous demagnetization of remanence during cooling. Knowledge of this expanded range of magnetic properties of greigite should be widely useful in environmental magnetic and paleomagnetic studies. **Citation:** Chang, L., A. P. Roberts, A. R. Muxworthy, Y. Tang, Q. Chen, C. J. Rowan, Q. Liu, and P. Pruner (2007), Magnetic characteristics of synthetic pseudo-single-domain and multi-domain greigite (Fe_3S_4), *Geophys. Res. Lett.*, *34*, L24304, doi:10.1029/2007GL032114.

1. Introduction

[2] Greigite (Fe_3S_4) is a ferrimagnetic iron sulfide mineral that forms in sulfate reducing conditions as a precursor to pyrite (FeS_2) in association with bacterial degradation of organic matter [*Berner*, 1984]. It is now recognized as a widespread magnetic mineral in many marine and lake sedimentary environments [e.g., *Roberts and Weaver*, 2005, and references therein]. The widespread occurrence of greigite makes understanding its magnetic properties important in many paleomagnetic and environmental magnetic studies [e.g., *Snowball*, 1991; *Rowan and Roberts*, 2006]. However, unlike its iron oxide spinel counterpart, magnetite (Fe_3O_4), whose magnetic properties are well established, the magnetic properties of greigite are relatively poorly known. For example, no systematic study of the pseudo-single-domain (PSD) and multi-domain (MD) magnetic properties and no grain size dependence of magnetic properties have been reported for greigite.

[3] Greigite commonly occurs in the single domain (SD) state in sediments [*Roberts*, 1995]. Rock magnetic results from Neogene marine sediments from eastern New Zealand demonstrate the widespread occurrence of superparamagnetic (SP) behavior in many greigite-bearing sediments [*Rowan and Roberts*, 2006]. This natural greigite has fine grain size of normally less than a few hundred nanometers. MD behavior has been occasionally reported for natural greigite. For example, *Hoffmann* [1992] reported greigite from a brown coal basin in the Czech Republic [*Krs et al.*, 1990] that has a grain size of 4–8 μm and MD-like magnetic properties. First-order reversal curve (FORC) measurements for a natural greigite sample from the same sequence (Figure 1c) provide evidence of a mixture of SD and MD grains [*Roberts et al.*, 2006]. Coarse-grained greigite with MD properties can therefore be preserved over geological timescales in some settings. Synthetic greigite has been reported to consist of fine grains, normally in the nanometer size range [e.g., *Uda*, 1965; *Dekkers and Schoonen*, 1996; *Chen et al.*, 2005], and are dominated by SP behavior [e.g., *Spender et al.*, 1972; *Roberts*, 1995]. However, no synthetic PSD/MD greigite has been reported in the literature due to difficulties in synthesizing large greigite particles. We report the first magnetic data for synthetic PSD/MD greigite and provide a domain state dependent magnetic property framework for synthetic and natural greigite.

2. Samples

[4] Greigite samples were synthesized using a new hydrothermal method [*Tang et al.*, 2007] by reacting iron chloride ($FeCl_3 \cdot 6H_2O$) with thiourea (CH_4N_2S) and formic acid (HCOOH) at 170°C for 8 hours. The black powders consist of pure crystalline greigite (details to be published elsewhere). Twenty-one batches of pure greigite were produced (S171–S711, Table 1), and subjected to magnetic measurements shortly after synthesis. Iron sulfide nodules, containing SD greigite, from the Valle Ricca section near Rome [*Florindo and Sagnotti*, 1995], and greigite-bearing Neogene marine sediments from eastern New Zealand, which contain variable mixtures of SP and stable SD properties [*Rowan and Roberts*, 2006], and a sample with mixed natural SD and MD greigite [*Roberts et al.*, 2006] from the Czech Republic (locality numbers 4077-81 (D16) given by *Krs et al.* [1990, Figure 1]) were also analysed to compare results with those from the synthetic PSD/MD

[1] National Oceanography Centre, University of Southampton, Southampton, UK.
[2] Department of Earth Science and Engineering, Imperial College London, London, UK.
[3] Hefei National Laboratory for Physical Sciences at Microscale and Department of Materials Science and Engineering, University of Science and Technology of China, Hefei, China.
[4] Institute of Geology, Academy of Sciences, Prague, Czech Republic.

0094-8276/07/2007GL032114$05.00

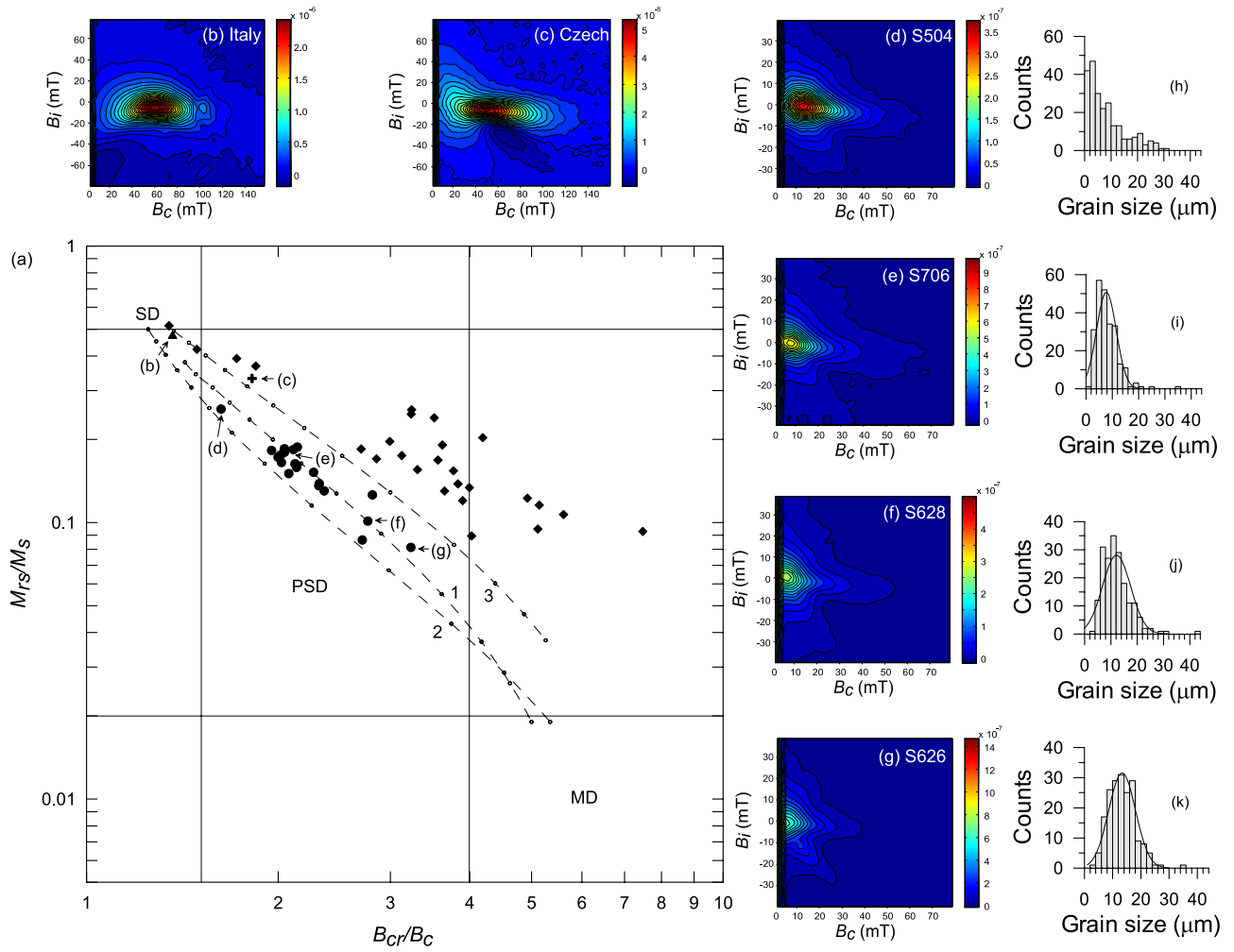

Figure 1. (a) Hysteresis data plotted after *Day et al.* [1977]. (b, c, d, e, f, g) FORC diagrams for samples in Figure 1a. (h, i, j, k) Grain size distributions for the synthetic greigite samples. Hysteresis ratios (solid circles) follow theoretical SD-MD mixing curves (1, 2 and 3; *Dunlop* [2002]). Decreasing M_{rs}/M_s and increasing B_{cr}/B_c are matched by increasing average grain size, consistent with progressive evolution of the FORC diagrams. Data for natural greigite samples are plotted for comparison. 'Italy' (triangle) is a typical natural SD sample (see Figure 1b) from a greigite-bearing nodule from the Valle Ricca section, near Rome, Italy [*Florindo and Sagnotti*, 1995]. 'Czech' (cross) is a natural greigite sample containing a mixture of SD, PSD, and MD grains (see Figure 1c) from the Czech Republic [cf. *Krs et al.*, 1990]. 'New Zealand' (solid diamonds) are Neogene marine sediments from eastern New Zealand that contain significant concentrations of SP grains, which follow SP-SD mixing curves [*Rowan and Roberts*, 2006].

samples, and to enable comparison of magnetic properties across a range of grain sizes for greigite.

3. Methods

[5] Hysteresis loops and back-field magnetizations were measured to determine the coercive force (B_c), the coercivity of remanence (B_{cr}), the saturation remanent magnetization (M_{rs}) and the saturation magnetization (M_s) using a Princeton Measurements Corporation vibrating sample magnetometer (VSM). FORCs were also measured on the VSM (140 FORCs per sample; averaging time = 200 ms) and FORC distributions were calculated based on the algorithm of *Pike* [2003] using a smoothing factor of 3 [*Roberts et al.*, 2000]. Low-temperature cycling (LTC) of a room-temperature (RT) saturation isothermal remanent magnetization (SIRM) (LTC-SIRM) and low-temperature (LT) SIRM warming after zero-field cooled (ZFC) and field cooled (FC) treatments were made with a Quantum Designs magnetic properties measurement system. For LTC-SIRM, the samples were imparted with a RT-SIRM; the remanence was then measured from RT to 10 K and back to RT in zero-field. For SIRM warming curves, samples were cooled to 10 K either in a 5 T field or in zero-field. A 5 T field was applied to the samples at 10 K and was switched off to impart a LT-SIRM. The remanence was then measured during warming in zero-field. Scanning electron microscope (SEM) observations were used to characterize the morphology and grain size (using a LEO 1450VP SEM, operated at 10–20 keV with an acceleration voltage of 17–20 pA). Grain size distributions were determined by measuring the

Table 1. RT Hysteresis Parameters of the Studied Greigite Samples

Samples	B_c, mT	B_{cr}, mT	M_{rs}/M_s	B_{cr}/B_c	Mean Grain Size, μm
S171	4.1	11.4	0.101	2.766	
S426	7.9	16.7	0.184	2.113	
S504	11.9	19.3	0.257	1.627	<4
S510	8.1	16.6	0.179	2.046	8.8 ± 4.6
S519	7.4	15.7	0.163	2.125	
S622	6.9	15.7	0.152	2.273	
S624	7.0	14.0	0.172	1.999	
S625	6.5	13.1	0.165	2.024	
S626	4.1	13.5	0.081	3.232	13.2 ± 4.5
S627	6.3	14.6	0.136	2.317	
S628	5.1	14.4	0.126	2.812	12.0 ± 4.8
S629	6.9	14.0	0.175	2.016	
S630	5.4	12.6	0.138	2.320	11.4 ± 5.3
S702	7.0	15.1	0.188	2.144	7.6 ± 3.7
S703	7.0	15.0	0.161	2.137	
S705	7.1	14.5	0.185	2.046	
S706	7.3	14.2	0.182	1.953	7.8 ± 3.8
S707	5.7	11.9	0.150	2.078	
S709	6.7	14.3	0.158	2.137	
S710	5.9	13.9	0.130	2.363	
S711	4.8	13.0	0.087	2.711	
Italy	49.9	68.1	0.478	1.365	
Czech	30.9	56.3	0.332	1.820	

long-dimension of ~200 grains for each sample (most grains are equi-dimensional).

4. Results

[6] RT hysteresis parameters (Table 1) indicate that the synthetic samples are magnetically soft compared with natural SD greigite samples [cf. *Roberts*, 1995]. Typical FORC diagrams for the studied synthetic samples (Figures 1g, 2c, 2d and 2e) have divergent contours, which are characteristic of MD behavior [e.g., *Roberts et al.*, 2000; *Pike et al.*, 2001]. In addition to MD-like behavior, samples at the finer end of the grain size spectrum (Figure 1h) have FORC distributions with concentric inner contours resembling those expected for PSD grains [*Roberts et al.*, 2000] (Figures 1d, 2a and 2b). As is the case for magnetite [*Roberts et al.*, 2000; *Muxworthy and Dunlop*, 2002], the FORC distribution peak shifts to lower coercivities (Figures 1d, 1e, 1f and 1g) as the mean grain size increases (Figures 1h, 1i, 1j and 1k). A FORC diagram for a greigite-bearing Miocene lacustrine sediment from the Czech Republic [*Krs et al.*, 1990], contains a peak in the FORC distribution at B_c ~60 mT (Figure 1c), with concentric and vertically spread inner contours and outermost contours that diverge rather than converge at lower coercivities, as would be expected for a MD distribution (Figure 1c). *Roberts et al.* [2006] interpreted this FORC diagram as containing evidence for bi-modal mixtures of SD and MD grains. The studied synthetic greigite samples extend these observations to coarser grain sizes, where the FORC diagrams consist of clearly divergent contours (Figures 1d, 1e, 1f and 1g), which suggest the dominance of PSD/MD particles. LT FORC distributions for selected PSD and MD synthetic samples are almost indistinguishable from RT FORC diagrams (Figure 2), unlike PSD magnetite, for which the FORC distribution splits into two sets of concentric contours at low temperatures [e.g., *Carvallo and Muxworthy*, 2006; *Smirnov*, 2006], which is probably associated with induced anisotropy effects [*Smirnov*, 2006]. It should be noted, however, that it is still unclear whether the observed splitting of the FORC distribution occurs across the entire PSD size range in magnetite. Nevertheless, the lack of a LT magnetic transition for greigite [e.g., *Spender et al.*, 1972; *Roberts*, 1995] could explain the LT stability of the FORC diagrams for PSD/MD greigite (Figure 2). LT FORC diagrams also provide further

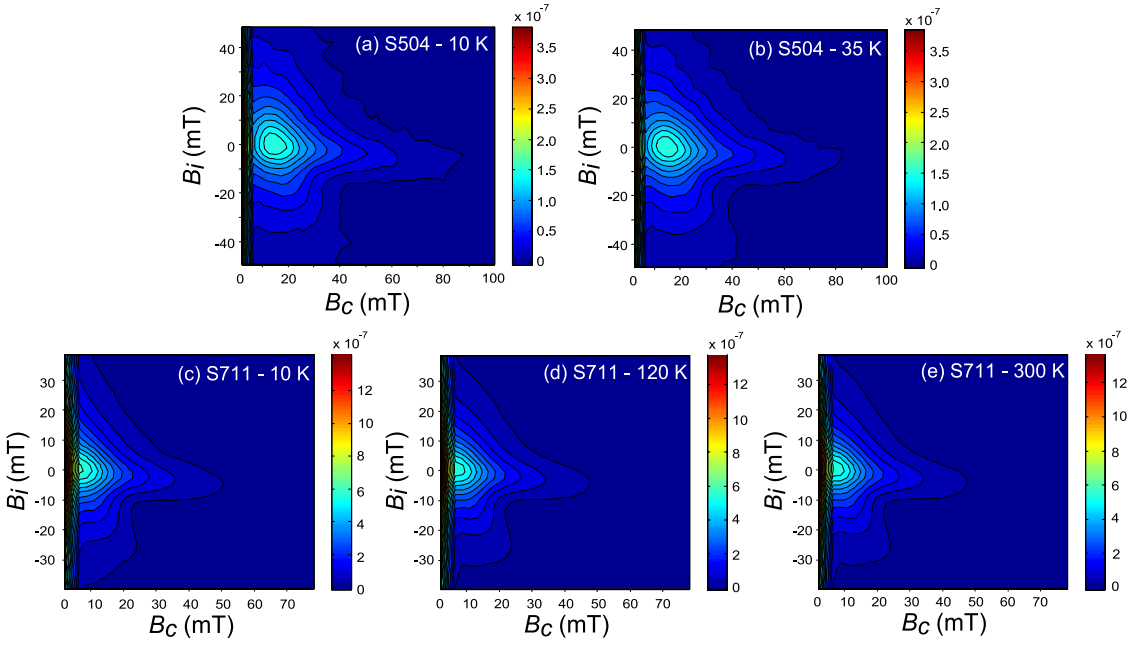

Figure 2. Low-temperature FORC diagrams for a dominantly PSD greigite sample (S504) at (a) 10 K and (b) 35 K; and for a dominantly MD greigite sample (S711) at (c) 10 K, (d) 120 K, and (e) 300 K.

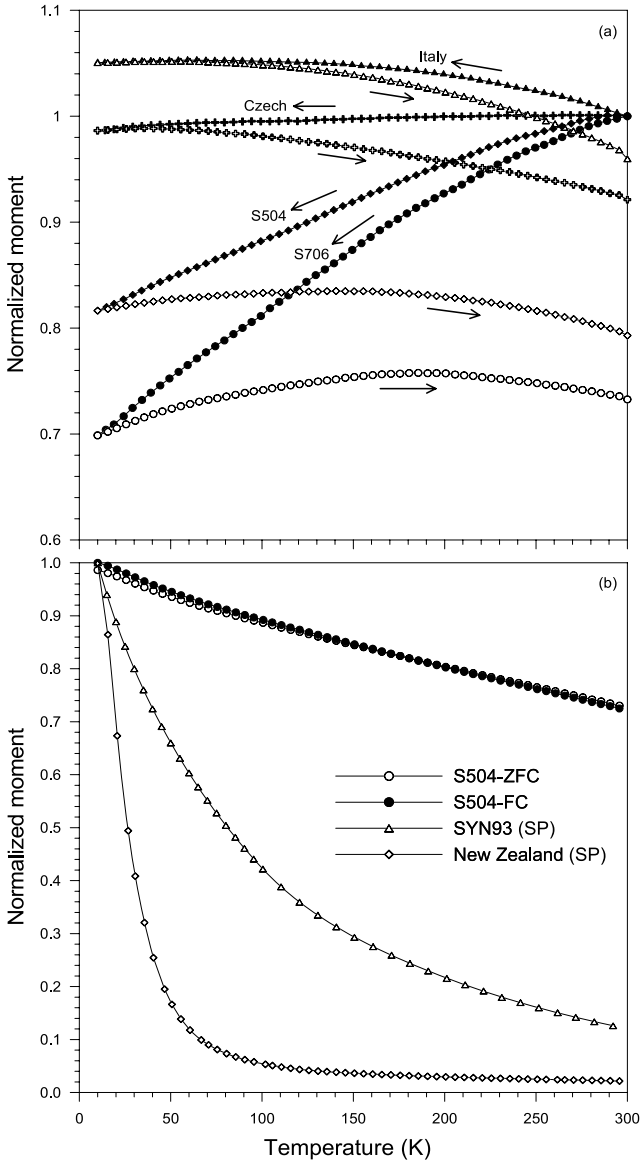

Figure 3. (a) Normalized zero-field cooling (solid symbols) and warming (open symbols) of SIRM for greigite samples. Circles, synthetic sample S706; diamonds, synthetic sample S504; triangles, 'Italy'; crosses, 'Czech'. (b) Normalized SIRM warming curves for synthetic greigite sample S504 during zero-field warming from 10 K to 300 K after ZFC (open circles) and FC (solid circles) treatments. SIRM warming curves are also plotted for a synthetic SP greigite sample (triangles) [*Roberts*, 1995, Figure 4] and for sedimentary greigite with dominant SP behavior from eastern New Zealand [*Rowan and Roberts*, 2006].

evidence that the low coercivities of these samples result from the presence of dominantly PSD/MD behavior rather than thermally activated SD behavior.

[7] Zero-field LTC (300 K → 10 K → 300 K) of a RT-SIRM (Figure 3a) reveals no discontinuities, unlike magnetite. The SIRM continuously demagnetizes during cooling from 300 to 10 K for the synthetic samples, and the remanence is irreversible during warming with respect to cooling. The remanence at RT after LTC for samples S706 and S504 is ~73% and 79% of the initial SIRM, respectively. For typical SD sedimentary greigite from Italy [*Florindo and Sagnotti*, 1995], SIRM gradually increases upon cooling from 300 to 10 K (Figure 3a), although upon warming the process is not completely reversible with respect to cooling, as SIRM gradually decreases to ~96% of the initial RT-SIRM value. The Czech Republic sample [*Krs et al.*, 1990; *Hoffmann*, 1992] with mixed MD and SD grains [*Roberts et al.*, 2006] has intermediate behavior between the SD and PSD/MD extremes during LTC (Figure 3a). In magnetite, demagnetization during ZFC of remanence (SIRM, anhysteretic remanence and/or thermoremanence) has been well documented [*Petrova and Trukhin*, 1961; *Markov et al.*, 1983] to depend on domain state; small SD grains do not demagnetize, while larger MD magnetite demagnetizes irreversibly upon cooling to above the Verwey transition. This irreversible demagnetization has been associated with domain re-ordering, i.e., domain wall re-equilibration or domain nucleation due to temperature-dependent changes in magnetocrystalline anisotropy and trans-domain processes [*Muxworthy et al.*, 2003]. The studied synthetic greigite samples undergo continuous demagnetization of SIRM during ZFC of LTC (Figure 3a). This decrease is probably due to identical PSD/MD processes that cause the remanence to decrease on cooling in magnetite. The observed demagnetization during LTC for the synthetic greigite samples provides further indirect evidence of the dominance of PSD/MD behavior. In contrast, almost no magnetic memory is lost for the Italian SD greigite sample. The remanence increase for SD samples during cooling is probably associated with the change in M_s with temperature.

[8] The lack of a LT transition or even a magnetic isotropic point (where the magnetocrystalline anisotropy is zero and changes signs) in LT-SIRM warming curves (Figure 3b) is consistent with the findings of *Moskowitz et al.* [1993] and *Roberts* [1995]. The synthetic PSD/MD greigite samples undergo a small remanence drop during warming, unlike greigite samples with substantial SP behavior, which undergo a large decrease in remanence [cf. *Roberts*, 1995, Figure 4]. The SIRM decrease for PSD/MD greigite during warming can be attributed to domain wall unpinning [*Moskowitz et al.*, 1998]. Sedimentary greigite from New Zealand with dominant SP behavior undergoes a large LT decrease in remanence (Figure 3b), in agreement with the interpretation of *Rowan and Roberts* [2006]. For magnetite, ZFC and FC SIRM warming curves diverge below the Verwey transition due to magnetocrystalline anisotropy re-orientation [e.g., *Moskowitz et al.*, 1993]. However, for greigite, which apparently has no crystallographic transition, the two curves overlap, which is consistent with the results of *Moskowitz et al.* [1993] for one natural greigite sample.

5. Discussion and Conclusions

[9] The studied synthetic greigite samples are dominated by PSD/MD magnetic behavior, as demonstrated with FORC diagrams, LTC-SIRM and LT-SIRM warming measurements. SEM observations reveal that the studied synthetic samples have a broad grain size distribution with a

maximum grain size of ~44 μm (Figures 1h–1k). Compared to magnetite, the observed grain-size ranges for the synthetic greigite samples span those expected for PSD and MD grains. On a Day plot [*Day et al.*, 1977], data for the synthetic samples fall on a trend calculated for mixtures of SD and MD magnetite [*Dunlop*, 2002], although strict numerical comparison between greigite and magnetite can not be made. By contrast, data from sedimentary greigite samples from New Zealand [*Rowan and Roberts*, 2006] follow a trend that resembles theoretical SP-SD mixing curves [*Dunlop*, 2002]. Differences in magnetic properties amongst the studied synthetic greigite samples are related to the different grain size distributions (Figures 1h–1k). Sample S626 (mean grain size $d = 13 \pm 5$ μm) has low M_{rs}/M_s (0.08) and high B_{cr}/B_c (3.23) values (Figure 1a), and the FORC distribution has clearly divergent contours (Figure 1g). By contrast, sample S504 ($d < 4$ μm) contains finer particles attached to the surface of large greigite crystals (Figure 1h) and yields higher M_{rs}/M_s (0.26) and lower B_{cr}/B_c (1.63) values (Figure 1a). The FORC distribution for this sample also contains concentric contours, which indicate the presence of PSD grains (Figure 1d). This is consistent with the relatively smaller fraction of remanence lost during LTC for sample S504 compared to sample S706 ($d = 8 \pm 4$ μm) (Figure 3a).

[10] This study demonstrates that synthetic PSD/MD greigite can be produced in the laboratory, just as coarse-grained sedimentary greigite can sometimes be preserved in natural environments [*Hoffmann*, 1992]. *Rowan and Roberts* [2006] found that SP behavior may be common in rapidly-deposited marine sediments, which means that use of classic SD properties to identify greigite [cf. *Roberts*, 1995] will lead to widespread underestimation of its presence in sediments. Likewise, our results for PSD/MD greigite indicate that its coercivity overlaps with that of PSD/MD magnetite and the lack of a LT transition in greigite can also overlap the LT behavior for maghemite or partially oxidized magnetite, which means that the presence of PSD/MD greigite in sediments is also likely to be underestimated unless additional high- and low-temperature measurements are made. Regardless, characterization of the full range of magnetic properties of greigite, to which this paper contributes, is necessary to enable identification of greigite in natural environments and will lead to a better understanding of greigite diagenesis. Such an improved understanding of the magnetic properties and occurrence of greigite will be important for a range of environmental magnetic and paleomagnetic studies.

[11] **Acknowledgments.** Liao Chang is supported by the U.K. Natural Environment Research Council. Greigite synthesis was supported by the National Natural Science Foundation of China (grants 20321101, 20125103 and 90206034). The Institute for Rock Magnetism, which is funded by the National Science Foundation, the Keck Foundation and the University of Minnesota, provided a visiting fellowship. Mike Jackson, Peat Sølheid and Brian Carter-Stiglitz helped with measurements. FORC data were processed with software produced by Michael Winklhofer. Sampling in the Czech Republic was part of project IAA3013406. Additional funding was provided by the Royal Society.

References

Berner, R. A. (1984), Sedimentary pyrite formation: An update, *Geochim. Cosmochim. Acta*, *48*, 605–615.

Carvallo, C., and A. Muxworthy (2006), Low-temperature first-order reversal curve (FORC) diagrams for synthetic and natural samples, *Geochem. Geophys. Geosyst.*, *7*, Q09003, doi:10.1029/2006GC001299.

Chen, X. Y., X. F. Zhang, J. X. Wan, Z. H. Wang, and Y. T. Qian (2005), Selective fabrication of metastable greigite (Fe_3S_4) nanocrystallites and its magnetic properties through a simple solution-based route, *Chem. Phys. Lett.*, *403*, 396–399.

Day, R., M. Fuller, and V. A. Schmidt (1977), Hysteresis properties of titanomagnetites: Grain size and composition dependence, *Phys. Earth Planet. Inter.*, *13*, 260–267.

Dekkers, M. J., and M. A. A. Schoonen (1996), Magnetic properties of hydrothermally synthesized greigite: I. Rock magnetic parameters at room temperature, *Geophys. J. Int.*, *126*, 360–368.

Dunlop, D. J. (2002), Theory and application of the Day plot (Mrs/Ms versus Hcr/Hc): 1. Theoretical curves and tests using titanomagnetite data, *J. Geophys. Res.*, *107*(B3), 2056, doi:10.1029/2001JB000486.

Florindo, F., and L. Sagnotti (1995), Palaeomagnetism and rock magnetism in the upper Pliocene Valle Ricca (Rome, Italy) section, *Geophys. J. Int.*, *123*, 340–354.

Hoffmann, V. (1992), Greigite (Fe_3S_4), magnetic properties and first domain observations, *Phys. Earth Planet. Inter.*, *70*, 288–301.

Krs, M., M. Krsová, P. Pruner, A. Zeman, F. Novák, and J. Jansa (1990), A petromagnetic study of Miocene rocks bearing micro-organic material and the magnetic mineral greigite (Sokolov and Cheb basins, Czechoslovakia), *Phys. Earth Planet. Inter.*, *63*, 98–112.

Markov, G. P., V. P. Shcherbakov, A. S. Bolshakov, and Y. K. Vinogradov (1983), On the temperature-dependence of partial thermoremanent magnetization in multidomain grains, *Izv. Akad. Nauk SSSR, Ser. Fiz.*, *19*, 625–630.

Moskowitz, B. M., R. B. Frankel, and D. A. Bazylinski (1993), Rock magnetic criteria for the detection of biogenic magnetite, *Earth Planet. Sci. Lett.*, *120*, 283–300.

Moskowitz, B. M., M. Jackson, and C. Kissel (1998), Low-temperature magnetic behavior of titanomagnetites, *Earth Planet. Sci. Lett.*, *157*, 141–149.

Muxworthy, A. R., and D. J. Dunlop (2002), First-order reversal curve (FORC) diagrams for pseudo-single-domain magnetites at high temperature, *Earth Planet. Sci. Lett.*, *203*, 369–382.

Muxworthy, A. R., D. J. Dunlop, and W. Williams (2003), High-temperature magnetic stability of small magnetite particles, *J. Geophys. Res.*, *108*(B5), 2281, doi:10.1029/2002JB002195.

Petrova, G. N., and V. I. Trukhin (1961), Spontaneous changes in H_c of particular cycles of magnetization observed during cooling of ferromagnetic minerals, *Izv. Phys. Solid Earth*, *6*, 584–588.

Pike, C. R. (2003), First-order reversal-curve diagrams and reversible magnetization, *Phys. Rev. B.*, 104424.

Pike, C. R., A. P. Roberts, M. J. Dekkers, and K. L. Verosub (2001), An investigation of multi-domain hysteresis mechanisms using FORC diagrams, *Phys. Earth Planet. Inter.*, *126*, 11–25.

Roberts, A. P. (1995), Magnetic characteristics of sedimentary greigite (Fe_3S_4), *Earth Planet. Sci. Lett.*, *134*, 227–236.

Roberts, A. P., and R. Weaver (2005), Multiple mechanisms of remagnetization involving sedimentary greigite (Fe_3S_4), *Earth Planet. Sci. Lett.*, *231*, 263–277.

Roberts, A. P., C. R. Pike, and K. L. Verosub (2000), FORC diagrams: A new tool for characterizing the magnetic properties of natural samples, *J. Geophys. Res.*, *105*, 28,461–28,475.

Roberts, A. P., Q. Liu, C. J. Rowan, L. Chang, C. Carvallo, J. Torrent, and C. S. Horng (2006), Characterization of hematite (α-Fe_2O_3), goethite (α-FeOOH), greigite (Fe_3S_4), and pyrrhotite (Fe_7S_8) using first-order reversal curve diagrams, *J. Geophys. Res.*, *111*, B12S35, doi:10.1029/2006JB004715.

Rowan, C. J., and A. P. Roberts (2006), Magnetite dissolution, diachronous greigite formation, and secondary magnetizations from pyrite oxidation: Unravelling complex magnetizations in Neogene marine sediments from New Zealand, *Earth Planet. Sci. Lett.*, *241*, 119–137.

Smirnov, A. V. (2006), Low-temperature magnetic properties of magnetite using first-order reversal curve analysis: Implications for the pseudo-single-domain state, *Geochem. Geophys. Geosyst.*, *7*, Q11011, doi:10.1029/2006GC001397.

Snowball, I. F. (1991), Magnetic hysteresis properties of greigite (Fe_3S_4) and a new occurrence in Holocene sediments from Swedish Lappland, *Phys. Earth Planet. Inter.*, *68*, 32–40.

Spender, M. R., J. M. D. Coey, and A. H. Morrish (1972), The magnetic properties and Mössbauer spectra of synthetic samples of Fe_3S_4, *Can. J. Phys.*, *50*, 2313–2326.

Tang, Y., Q. W. Chen, Y. Xiong, and Y. Li (2007), Magnetic field-induced increase in conversion rate of Fe_3S_4 to FeS_2, *Chin. J. Inorg. Chem.*, *23*, 941–947.

Uda, M. (1965), On the synthesis of greigite, *Am. Mineral.*, *50*, 1487–1489.

L. Chang, Q. Liu, A. P. Roberts, and C. J. Rowan, National Oceanography Centre, University of Southampton, European Way, Southampton SO14 3ZH, UK. (changl@noc.soton.ac.uk)

Q. Chen and Y. Tang, Hefei National Laboratory for Physical Sciences at Microscale and Department of Materials Science and Engineering, University of Science and Technology of China, Hefei 230026, China.

A. R. Muxworthy, Department of Earth Science and Engineering, Imperial College London, South Kensington Campus, London SW7 2AZ, UK.

P. Pruner, Institute of Geology, Academy of Sciences, Rozvojová 135, Prague CZ-16502, Czech Republic.